

Detection of the phenomenon of turbulent thermal diffusion in numerical simulations

Nils Erland L. Haugen,^{1,*} Nathan Kleeorin,^{2,†} Igor Rogachevskii,^{2,‡} and Axel Brandenburg^{3,4,§}

¹*SINTEF Energy Research, N-7034 Trondheim, Norway*

²*Department of Mechanical Engineering, Ben-Gurion University of the Negev, P.O.Box 653, Beer-Sheva 84105, Israel*

³*NORDITA, AlbaNova University Center, Roslagstullsbacken 23, SE-10691 Stockholm, Sweden*

⁴*Department of Astronomy, Stockholm University, SE 10691 Stockholm, Sweden*

(Dated: March 13, 2019, Revision: 1.78)

The phenomenon of turbulent thermal diffusion in temperature-stratified turbulence causing a non-diffusive turbulent flux of inertial particles in the direction of the turbulent heat flux, is found using direct numerical simulations (DNS). In simulations with and without gravity, a peak in the particle number density is found around the minimum of the mean fluid temperature for Stokes numbers less than 1 due to the phenomenon of turbulent thermal diffusion, where the Stokes number is the ratio of particle Stokes time to turbulent Kolmogorov time at the viscous scale. This phenomenon causes formation of large-scale inhomogeneities in the spatial distribution of inertial particles. For Stokes numbers larger than 1, this effect decreases with increasing Stokes number.

PACS numbers: 47.27.tb, 47.27.T-, 47.55.Hd, 47.55.Kf

Transport and mixing of small particles (aerosols and droplets) in turbulent fluid flow is of fundamental significance in a large variety of applications (environmental sciences, physics of the atmosphere and meteorology, industrial turbulent flows and turbulent combustion, see, e.g., [1, 2]). Turbulent diffusion causes destruction of large-scale inhomogeneities in the spatial distributions of particles. The opposite effect, turbulent thermal diffusion in temperature-stratified turbulence [3], can cause the formation of inhomogeneous structures in the particle density in the vicinity of the mean temperature minimum due to the appearance of a turbulent non-diffusive flux of inertial particles in the direction of the turbulent heat flux. The phenomenon of turbulent thermal diffusion has been predicted theoretically in [3] and detected in different laboratory experiments in stably and unstably temperature-stratified turbulence [4–6]. This phenomenon is shown to be important for the atmospheric turbulence with temperature inversions [7] and for small-scale particle clustering in temperature-stratified turbulence [6], but it is also expected to be of large significance for different kinds of heat exchangers (e.g., industrial boilers where the Reynolds numbers and temperature gradients are large). In spite of the fact that turbulent thermal diffusion has already been found in different types of laboratory experiments and atmospheric flows, this effect has never been observed in direct numerical simulations (DNS). The main goal of this Letter is to describe the detection of the phenomenon of turbulent thermal diffusion in DNS.

In order to study the formation of inhomogeneous particle structures, the equation for the total particle number density is averaged over an ensemble of turbulent velocity fields. This yields the equation for the mean number density, N , of particles that has been derived

using different approaches in [3, 7–10]:

$$\frac{\partial N}{\partial t} + \nabla \cdot [N (\mathbf{W}_g + \mathbf{V}^{\text{eff}}) - D_T \nabla N] = 0, \quad (1)$$

where $\mathbf{V}^{\text{eff}} = -\tau_f \overline{\mathbf{U}_p (\nabla \cdot \mathbf{U}_p)} = -\alpha D_T \nabla \bar{T} / \bar{T}$ is the effective particle velocity due to turbulent thermal diffusion, \mathbf{U}_p is the particle velocity, \bar{T} is the mean fluid temperature, D_T is the turbulent diffusion coefficient, τ_f is the fluid turbulent integral timescale, overbars imply ensemble averaging, $\mathbf{W}_g = \tau_p \mathbf{g}$ is the terminal fall velocity of particles, \mathbf{g} is the gravitational acceleration, τ_p is the Stokes time that describes the particle-fluid interactions. The coefficient $\alpha = 1$ for non-inertial particles, while for inertial particles α depends on τ_p and the fluid Reynolds number [3, 7]. Equation (1) is written for a zero mean fluid velocity. The non-diffusive mean flux of particles, $N \mathbf{V}^{\text{eff}}$, that is directed toward the mean temperature minimum, is the main reason for the formation of large-scale inhomogeneous distributions of inertial particles in temperature-stratified turbulence. Indeed, the steady-state solution of Eq. (1) for the mean number density of inertial particles is given by

$$\tilde{N}(z) = [\tilde{T}(z)]^{-\alpha} \exp \left[- \int_{z_0}^z [W_g / D_T] dz' \right], \quad (2)$$

where $W_g = |\mathbf{W}_g|$, the non-dimensional mean temperature is defined as $\tilde{T} = \bar{T} / \bar{T}_0$, while the non-dimensional mean number density of particles is $\tilde{N} = N / N_0$, where the subscripts 0 represent the values at the boundary. Equation (2) implies that small particles are accumulated in the vicinity of the mean temperature minimum.

The mechanism of turbulent thermal diffusion for inertial particles with material density much larger than the fluid density, is as follows [3]. The inertia causes particles inside the turbulent eddies to drift out to the boundary regions between eddies. These regions have

low vorticity, high strain rate and maximum fluid pressure [11]. There is also an outflow of particles from regions with minimum fluid pressure. In homogeneous and isotropic turbulence without mean gradients of temperature, a drift from regions with increased concentration of particles by a turbulent flow is equiprobable in all directions, and the pressure (temperature) of the surrounding fluid is not correlated with the turbulent velocity field. In temperature-stratified turbulence, fluctuations of fluid temperature and velocity are correlated due to a non-zero turbulent heat flux. Fluctuations of temperature cause pressure fluctuations, which result in fluctuations of the number density of particles. Increase of the pressure of the surrounding fluid is accompanied by an accumulation of particles, and the direction of the mean flux of particles coincides with that of the turbulent heat flux. The mean flux of particles is directed toward the minimum of the mean temperature, and the particles tend to be accumulated in this region [3, 7, 8].

In the present study equations for the fluid are solved by employing DNS in an Eulerian framework, while the equation of motion of the particles is solved in a Lagrangian framework. All numerical simulations have been performed using the Pencil Code [12] (for details of the code, see Refs. [13, 14]). The set of compressible hydrodynamic equations is solved for the fluid density ρ , the fluid velocity \mathbf{U} , and the specific entropy s :

$$\frac{D \ln \rho}{Dt} = -\nabla \cdot \mathbf{U}, \quad (3)$$

$$\frac{D \mathbf{U}}{Dt} = -\frac{1}{\rho} [\nabla p - \nabla \cdot (2\rho\nu\mathbf{S})] + \mathbf{f}, \quad (4)$$

$$T \frac{Ds}{Dt} = \frac{1}{\rho} \nabla \cdot K \nabla T + 2\nu \mathbf{S}^2 - c_P (T - T_{\text{ref}}), \quad (5)$$

where T is the fluid temperature, c_P is the specific heat, $D/Dt = \partial/\partial t + \mathbf{U} \cdot \nabla$ is the advective derivative, \mathbf{f} is the external forcing function, p is the fluid pressure, ν is the kinematic viscosity, and K is the coefficient of the thermal conductivity. The traceless rate of strain tensor is given by $\mathbf{S}_{ij} = \frac{1}{2}(U_{i,j} + U_{j,i}) - \frac{1}{3}\delta_{ij}\nabla \cdot \mathbf{U}$, where $U_{i,j} = \nabla_j U_i$. The last term in the entropy equation (5) determines the cooling, which causes the fluid temperature minimum at $z = 0$, where $T_{\text{ref}} = T_0 + \delta T \exp(-z^2/2\sigma^2)$, z is the spatial position in the vertical direction, and T_0 is the mean temperature far from the cooled zone. The size of the simulation domain is $L = 2\pi$ in all three directions and the width of the cooling function is $\sigma = 0.5$. Furthermore the strength of the cooling function, δT , is such that the relative contrast between temperature maximum and temperature minimum is ~ 1.6 . In all simulations the Prandtl number is unity. Turbulence in the simulation box is produced by the forcing function, \mathbf{f} , which injects energy along a wavevector whose direction changes every timestep, but its length is approximately k_f (see [15]). The strength of the forcing is set such that the maximum Mach number is below 0.5. It has been

checked that decreasing the Mach number by a factor of 5 does not have any significant effect on the results.

Particles are treated as point particles and we consider the one-way coupling approximation, i.e., there is an effect of the fluid on the particles only, while the particles do not influence the fluid motions. This is a good approximation when the spatial density of particles is much smaller than the fluid density. The particle equation of motion is solved

$$d\mathbf{U}_p/dt = \mathbf{g} - \tau_p^{-1}(\mathbf{U}_p - \mathbf{U}), \quad (6)$$

where $d\mathbf{X}/dt = \mathbf{U}_p$, $\tau_p = Sd^2/[18\nu(1-f_c)]$ is the Stokes time, $f_c = 0.15\text{Re}_p^{0.687}$ [2], d is particle diameter and $\text{Re}_p = |\mathbf{U}_p - \mathbf{U}|d/\nu$ is the particle Reynolds number. The key parameter of the problem is the Stokes number $\text{St} = \tau_p/\tau_k$ that is based on the particle Stokes time and the Kolmogorov timescale $\tau_k = \tau_f/\sqrt{\text{Re}}$, where $\tau_f = 1/u_{\text{rms}}k_f$ is the turbulent integral timescale, $\text{Re} = u_{\text{rms}}/\nu k_f$ is the fluid Reynolds number and u_{rms} is the root mean square velocity. The parameter f_c is used for inertial particles with $\text{Re}_p \geq 1$. The ratio between the particle material density and the fluid mass density is $S = \rho_p/\rho$ and for all simulations $S = 1000$ outside the cooled zone. It has been checked that adding small Brownian diffusion of particles does not affect the results. For all simulations the number of Eulerian grid points are 128^3 , while the number of Lagrangian particles is 5×10^5 . It has been verified that increasing the number of grid points or the number of particles has no effect on the results.

In simulations without gravity, periodic boundary conditions are used in all directions both for the fluid and for the particles. When gravity is taken into account in simulations, particles are made elastically reflecting from the vertical boundaries. In all our simulations, gravity is ignored in Eq. (4) for the fluid, but it is included in Eq. (6) for particle motions. This situation has direct applications to atmospheric turbulence with lower-troposphere temperature inversions, where the density scale height due to the gravity is about 8 km, while the characteristic temperature inhomogeneity scale inside the temperature inversions is about 500–800 m, and the integral scale of turbulence is about 50–100 m.

Let us first discuss the results of the numerical simulations of formation of the particle inhomogeneous structures in the absence of gravity. In Fig. 1 we plot the vertical profile of the mean number density of particles for simulations with $k_f = 5$, $\text{Re} = 240$ and different Stokes numbers. Inspection of Fig. 1 shows that the maximum in the particle number density is located in the vicinity of the mean temperature minimum for a wide range of the Stokes numbers. In the absence of gravity ($\mathbf{W}_g = 0$), the parameter α is given by $\alpha = -\ln \tilde{N}/\ln \tilde{T}$ [see Eq. (2)]. In Fig. 2 the Stokes number dependence of the parameter α is shown for different Reynolds numbers and different forcing scales. It can be seen that the parameter

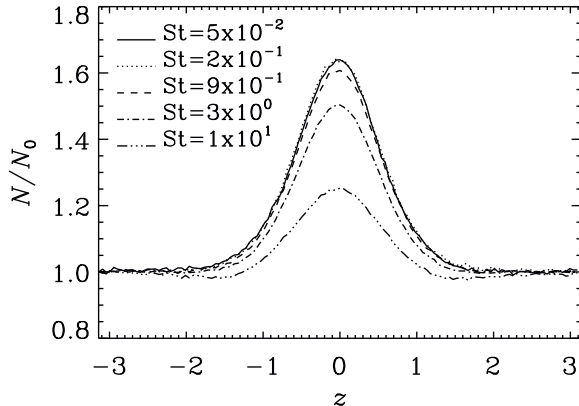


FIG. 1. Vertical profile of the mean number density for different Stokes numbers for simulations with $k_f = 5$, $Re = 240$ when the kinematic viscosity is kept constant and no gravity.

α reaches its maximum value for $St_* \approx 0.2$, while for Stokes numbers $St > St_*$, the value of α decreases monotonically. A critical Stokes number, St_c , separating the large and small Stokes number regimes might be defined such that $\alpha \geq 1$ for $St < St_c$, while for $St > St_c$ the parameter α is decreasing steeply with increasing Stokes number. Since in the simulations the rms Mach number is not very small (around 0.2), the maximum value of the parameter α is slightly larger than 1. Decreasing the Mach number causes α to increase due to particle inertia, e.g., in the atmospheric turbulence the Mach number is of the order of $(0.1 - 3) \times 10^{-3}$ and α is about 10 [7]. Large particles with $\tau_p \sim \tau_f$ are affected primarily by the largest turbulent eddies in the flow. This is because the smaller turbulent eddies have turnover times much shorter than the particle's Stokes time, and they cannot accelerate the particles. The parameter α for the large particles decreases strongly with $\tau_p \propto St$ (see Fig. 2 in the large Stokes number regime). Furthermore, it is expected that, in the large Stokes number regime, α is independent of Re as long as u_{rms} and k_f are kept constant. Since the Stokes number is based on the Kolmogorov time τ_k , this implies that $St_c \propto \sqrt{Re}$, which is indeed what is found in Fig. 2.

When experiencing a high fluid density a particle in the large Stokes number regime will more easily be accelerated by turbulence if ν is constant than if the dynamic viscosity $\mu = \rho\nu$ is constant. This is due to the fact that for constant ν a high fluid density is associated with a smaller Stokes number, while for constant μ the Stokes number is independent of fluid density. Due to this it is expected that particles with large Stokes numbers will tend to be more depleted from the high density regions when ν is constant than when μ is constant. This explains why the simulation shown in Fig. 2 with constant

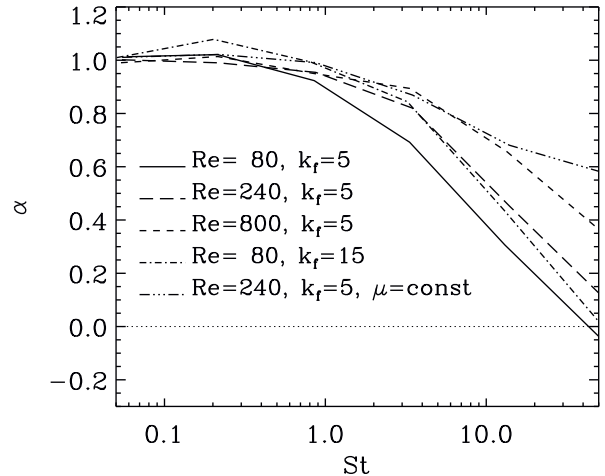


FIG. 2. The parameter α versus the Stokes number St for different Reynolds numbers and forcing wavenumbers in the absence of gravity. For the dashed-triple-dotted line the dynamic viscosity, $\mu = \rho\nu$, is kept constant while for all other lines the kinematic viscosity ν is kept constant.

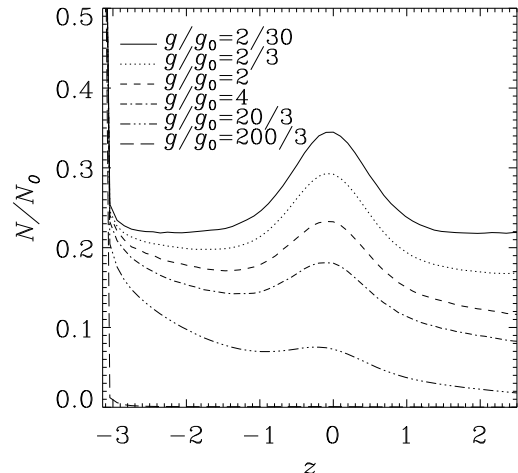


FIG. 3. Vertical profile of the mean number density for different gravitational accelerations, $St = 1$ and $k_f = 5.1$.

μ have a much shallower fall-off with increasing Stokes number in the large Stokes number regime than the simulations with constant ν .

If the integral scale of turbulence is close to the scale of the thermal cooling, a particle trapped inside a turbulent eddy might travel across the whole cooled zone during one eddy turnover time. This will effectively smear out the peak of the particle number density, and consequently also decrease the parameter α . For simulations with $k_f = 5$, the integral scale is comparable to the cooling scale, and the peak of α for $k_f = 5$ is lower than for simulations

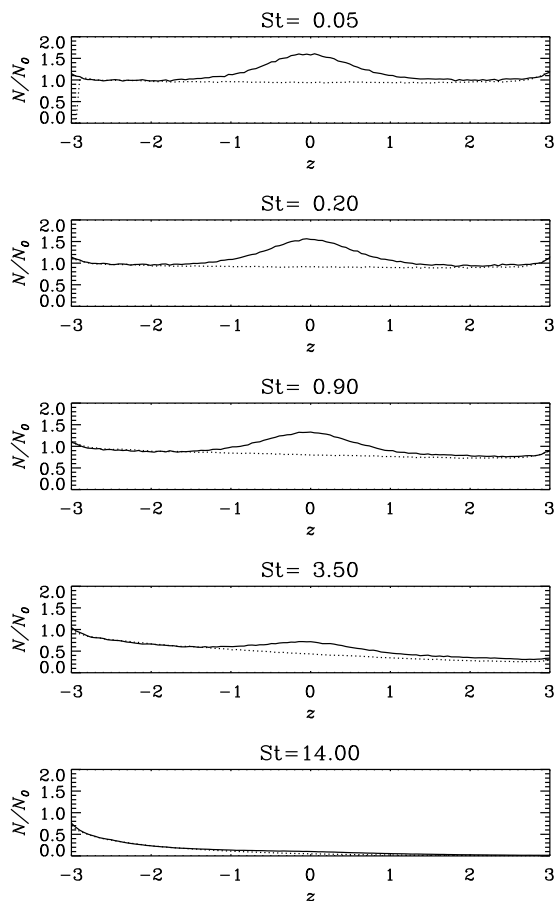


FIG. 4. Vertical profile of the mean number density (solid line) for $g/g_0 = 2/3$, $k_f = 5$ and different Stokes numbers. The dotted line represent the isothermal reference case.

with $k_f = 15$ (see Fig. 2). This trend is expected to continue for yet smaller k_f .

For larger Stokes numbers, gravity plays a crucial role, and must be included in the simulations. In Fig. 3, the mean particle number density is shown as a function of vertical position z for simulations with $St = 1$, $k_f = 5$, and different gravitational accelerations. In the following, gravity is nondimensionalized with $g_0 = D_T/(\tau_p L)$, so that $g/g_0 = L/L_g$, where $L_g = D_T/W_g$ is the characteristic scale of the mean particle number density variations due to the gravity for an isothermal case, $D_T = u_{rms}/3k_f$ is the turbulent diffusion coefficient, and L is the height of the box. As the particle sedimentation velocity is increased, the particle number density profile is more and more tilted, as expected. For large particle sedimentation velocity ($g/g_0 = 200/3$), almost all particles have accumulated at the lower wall (see Fig. 3). In Fig. 4, the vertical profile of the particle number density is shown for $g/g_0 = 2/3$ and different Stokes numbers. By fitting these results with Eq. (2), the parameter α is found to be about 1 for the three smallest Stokes numbers in Fig. 4, while for $St = 3.5$ and $St = 14$ a best fit

of α is found around 0.8 and 0.5, respectively. For large Stokes numbers the maximum particle number density is found near the bottom wall of the box due to the large sedimentation velocity.

In conclusion, our numerical simulations have demonstrated the existence of the phenomenon of turbulent thermal diffusion for different Stokes numbers, fluid Reynolds numbers and different forcing scales of turbulence. Furthermore the effect of gravity has been included in simulations. It has been shown that due to the effect of turbulent thermal diffusion, particles are accumulated in the vicinity of the mean fluid temperature minimum for $St < 1$ – in agreement with theoretical studies [3, 8], laboratory experiments [4–6] and the atmospheric observations [7]. When $St > 1$, this effect is decreasing with Stokes number.

This work was supported in part by the Norwegian Research Council project PAFFrx (186933) (NELH), and by the European Research Council under the AstroDyn Research Project 227952 (AB).

* Nils.E.Haugen@sintef.no

† nat@bgu.ac.il

‡ gary@bgu.ac.il

§ brandenb@nordita.org

- [1] A. K. Blackadar, *Turbulence and Diffusion in the Atmosphere* (Springer, Berlin, 1997).
- [2] C. T. Crowe, J. D. Schwarzkopf, M. Sommerfeld and Y. Tsuji, *Multiphase flows with droplets and particles*, second edition (CRC Press LLC, NY, 2011).
- [3] T. Elperin, N. Kleeorin and I. Rogachevskii, Phys. Rev. Lett. **76**, 224 (1996); Phys. Rev. E **55**, 2713 (1997).
- [4] J. Buchholz, A. Eidelman, T. Elperin, G. Grünefeld, N. Kleeorin, A. Krein, I. Rogachevskii, Experim. Fluids **36**, 879 (2004).
- [5] A. Eidelman, T. Elperin, N. Kleeorin, I. Rogachevskii and I. Sapir-Katiraie, Experim. Fluids **40**, 744 (2006).
- [6] A. Eidelman, T. Elperin, N. Kleeorin, B. Melnik and I. Rogachevskii, Phys. Rev. E **81**, 056313 (2010).
- [7] M. Sofiev, V. Sofieva, T. Elperin, N. Kleeorin, I. Rogachevskii and S. S. Zilitinkevich, J. Geophys. Res. **114**, D18209 (2009).
- [8] T. Elperin, N. Kleeorin, I. Rogachevskii and D. Sokoloff, Phys. Rev. E **61**, 2617 (2000); *ibid* **64**, 026304 (2001).
- [9] R. V. R. Pandya and F. Mashayek, Phys. Rev. Lett. **88**, 044501 (2002).
- [10] M. W. Reeks, Int. J. Multiph. Flow **31**, 93 (2005).
- [11] M. R. Maxey, J. Fluid Mech. **174**, 441 (1987).
- [12] The Pencil Code is a high-order finite-difference code (sixth order in space and third order in time); <http://pencil-code.googlecode.com>.
- [13] Johansen, A., Oishi, J. S., Mac Low, M. M., Klahr, H., Henning, T., & Youdin, A., Nature **448**, 1022 (2007).
- [14] N. E. L. Haugen and S. Kragset, J. Fluid Mech. **661**, 239-261 (2010).
- [15] N. E. L. Haugen and A. Brandenburg, Phys. Fluids **18**, 075106 (2006).